

2. P. Bussieres and A. C. Leonard, *Int. Inst. Refrig., Annexe*, 5, 61-84 (1966).
3. R. C. Steed and R. K. Irey, *Adv. Cryogen. Eng.*, 15, 299-307 (1970).
4. A. C. Leonard, *ICEC-3*, 109-114 (1970).
5. E. V. Ametistov, V. V. Zyatkevich, and V. U. Sidyganov, *Boiling and Condensation [in Russian]*, Riga (1982), pp. 94-100.
6. H. Kobayashi and K. Yasukoshi, *Cryogenics*, 19, No. 2, 93-96 (1979).
7. H. Kobayashi and K. Yasukoshi, *Cryogen. Eng. Conf.*, 1979, Paper FE-G, pp. 372-377.

CONDITIONS AND RATES OF HEAT TRANSFER DURING VAPORIZATION ON PROFILED SURFACES

O. G. Burdo

UDC 536.423.1

A relationship is given for calculating heat transfer during evaporation and boiling on profiled heating surfaces.

The problem of organizing vaporization processes on profiled heat-exchange surfaces is a timely one for various types of industrial equipment, and in particular in heat pipes of the so-called channel-capillary construction. The interest in such surfaces and their application for the intensification of transfer processes began a considerable time ago, since here microfilm evaporation is combined with acceptable hydrodynamic parameters (which are more favorable than in the case of porous structures.) However, the wide and effective introduction of profiled surfaces has not been possible because of the lack of information on the heat and mass transfer behavior under various conditions. Further extension of the investigations into transfer processes on channel-capillary structures facilitated carrying out work on heat pipes. The main results of this work can be characterized as follows.

1. The flow of the liquid has been determined to be laminar in channels of normal geometrical shapes under the influence of surface forces and the forces of gravity and friction, with the formation of menisci of cylindrical shapes [1-8].

2. The maximum heat flux is fixed by the known hydrodynamic limits on the operation of the heat pipe [1, 3, 6, 9].

3. There is no consensus of opinion as to the possible heat-transfer regimes or on the boundaries for the transition from one regime to another. The assumption that there is boiling of the liquid in the grooves is made in [6], and this is used as the basis for explaining the high heat-transfer rates. It is noted in [1] that boiling is not very probable in channels of such small dimensions, but on the other hand it was shown on the basis of an actual physical model that a high heat-transfer intensity can also be achieved during evaporation. Temperature fluctuations of the surface of an arterially grooved heat pipe with amplitudes of 150-250°K were noted in [6]. As the heat flux increased, the frequency of the fluctuations also increased, and then the fluctuations were no longer observed. The author did not explain the reason for the pulsations.

4. Even for the simplest evaporation regime there are essentially no experimental, design-analytical, or empirical relationships for calculating the thermal resistance which cover the ranges of the main factors needed in practice. The results of the experimental investigations have been treated differently by the authors, and the known solutions [1-4, 10-12] and the data on the thermal resistances of profiled surfaces [3-5, 7, 12] are of a partial nature only.

A group of investigations of the heat transfer processes in open capillary channels carried out in the OTIPP [Technological Institute of the Food Industry, Odessa] has shown that three vaporization regimes are possible: evaporative, evaporative-pulsating (quasievaporative), and boiling. The occurrence and coexistence of these regimes are governed mainly by the value of the heat flux, the heat-transfer medium, and the geometry of the surface. The evaporative regime has been stably observed on the plate L1 (Table 1), for which the length

M. V. Lomonosov Technological Institute of the Food Industry, Odessa. Translated from *Inzhenerno-Fizicheskii Zhurnal*, Vol. 52, No. 6, pp. 899-906, June, 1987. Original article submitted March 27, 1986.

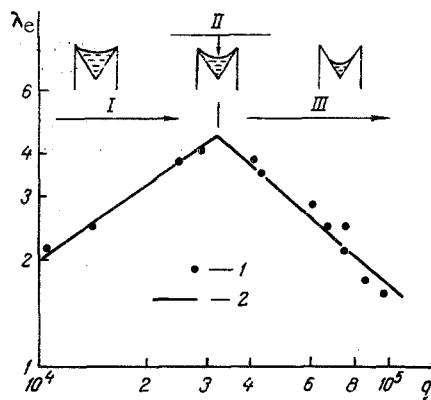


Fig. 1

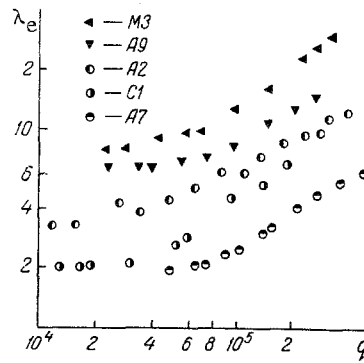


Fig. 2

Fig. 1. Effect of the heat flux on the value of the local coefficient of effective thermal conductivity; evaporation of water at $P = 0.1$ MPa. I) Decrease of the radius of curvature of the meniscus; II) meniscus just re-entrant; III) deepening of the meniscus and drying-out of the groove. 1) Experiment on plate L1; 2) calculation by (2). λ_e is given in $W/m \cdot K$ and q in W/m^2 .

Fig. 2. Effect of the heat flux on the value of the effective thermal conductivity of a capillary channel; evaporative-pulsating regime and boiling.

of the channels of the transport section was 150 mm and the length of the heating zone was 50 mm. On increasing the heat-flux density from $5 \cdot 10^3$ to $3.8 \cdot 10^4$ W/m^2 there was a decrease in the radius of curvature of the meniscus, which governed the increase in the local value of the coefficient of effective thermal conductivity of the channel (Fig. 1). A further increase in the heat flux and in the deepening of the meniscus led to a partial drying-out of the channel, and as a result, to a reduction in λ_e (Fig. 1).

Heat transfer during evaporation was studied over the range of ratios λ_L/λ_M from 10^{-4} to $3.8 \cdot 10^{-2}$ using the electrothermal analogy method. It was shown that the thermal resistance of the channel can be determined as the sum of the thermal resistances connected in series of the metallic base, the wetted channel, and the layer of liquid [13]. Evaluation of the data was carried out on the basis of various types of models, including those in which the transfer of heat through the wetted groove was represented as a process of heat conduction through a fin of the corresponding profile with a variable heat transfer coefficient [13]. Generalized relationships were obtained as a result of the modeling [14], and for specific combinations of the material of construction and the heat transfer medium the following simple approximations have been proposed:

for rectangular channels:

$$\lambda_e = \lambda_L \frac{s}{t} \left[1 + C_1 \left(\frac{s}{t} \sqrt{\frac{h}{s}} \right)^m \right] \exp \left(0.58 \frac{s}{R} \sqrt{\frac{s}{h}} \right), \quad (1)$$

for triangular channels:

$$\lambda_e = \lambda_L (a - b \sin \alpha) \exp \left(0.58 \frac{s}{R} \sqrt{\frac{s}{h}} \right). \quad (2)$$

The constants in Eqs. (1) and (2) depend on the ratio λ_L/λ_M . When $0.03 \leq \lambda_L/\lambda_M \leq 0.04$, $C_1 = 1.58$, $m = 1.64$, $a = 0.112$, $b = 0.059$. When $0.002 \leq \lambda_L/\lambda_M \leq 0.004$, $C_1 = 2.6$, $m = 1.5$. When $0.0005 \leq \lambda_L/\lambda_M \leq 0.0008$, $C_1 = 1.6$, $m = 1.5$, $a = 0.006$, $b = 0.0048$. The change of R over the length of the channel is governed by the heat flux and by the action of the gravity and surface tension forces.

During laminar flow of the liquid in the channels, the equation for the conservation of momentum can be written as

TABLE 1. Parameters of the Working Sections

A. Plates with rectangular grooves							
Surface	<i>h</i> , mm	<i>s</i> , mm	<i>t</i> , mm	Surface	<i>h</i> , mm	<i>s</i> , mm	<i>t</i> , mm
A1	0,15	0,1	0,3	A-6	0,50	0,1	0,4
A2	0,30	0,1	0,3	A-7	0,15	0,1	0,2
A3	0,50	0,1	0,3	M-1	0,50	0,2	0,4
A4	0,15	0,1	0,4	M-2	0,50	0,6	1,0
A5	0,30	0,1	0,4	C-1	0,50	0,7	1,0

B. Plates with trapezoidal channels			
Surface	<i>h</i> , mm	<i>s</i> , mm	Angle of vertex
A8	0,5	0,45	48°30'
A9	0,5	0,58	60°
M3	0,8	0,65	44°12'
LI	0,36	0,42	45°

Notes. A) Aluminum; M) copper; C) stainless steel; L) brass.

$$-\frac{\sigma}{R^2} \frac{dR}{dx} = c_f \frac{1}{d_e^2} \rho_L \frac{w}{2} \pm (\rho_L - \rho_v) g \sin \beta. \quad (3)$$

Here the equations for the conservation of mass and energy have the forms:

$$\rho_L f \frac{dw}{dx} + \rho_L w \frac{df}{dx} = j, \quad (4)$$

$$j(r + c_L \Delta t) = q - q_{\text{loss}}. \quad (5)$$

Assuming that the thermophysical properties of the liquid are independent of the temperature, and using the equivalent diameter $d_e = 4f/\pi$, with the boundary conditions

$$x=0 \quad w = \frac{Q}{r \rho_L f_0 n}, \quad (6)$$

$$x=l \quad w=0,$$

Eqs. (3)-(5) can be reduced to the form

$$-\frac{\sigma}{R^2} \frac{dR}{dx} = \frac{2v_L Q \Pi^2}{r n f_0^3}. \quad (7)$$

In writing Eq. (7) the assumptions are made that the meniscus is cylindrical in shape, and that the hydraulic diameter can be used as the characteristic dimension of the channel. These assumptions have been confirmed well by comparing the calculated and experimental data on the maximum heat fluxes [1, 3, 6, 9].

The determination of the curvature of the meniscus form (7) is necessary, as can be seen from (1) and (2), in order to calculate the local value of λ_e . The simultaneous solution of Eqs. (1), (2), and (7) is necessary. No examples of such calculations are known, and in a number of cases the determination of λ_e plays a role of exclusive importance. Figure 1 shows a comparison of calculations according to Eqs. (2) and (7) (allowing for the real geometry and operating conditions) with the data from experiments. The correctness of the thermal model for the evaporative regime can be noted, as well as the fact that it is possible to calculate it from the relationships (1) and (2).

The evaporative-pulsating regime was observed on plates A1-A9, C1, and M1-M3 (see Table 1). A description of the experimental equipment and of the main results is given in [15]. The experiments were characterized by concentration of the heat fluxes by means of a heat

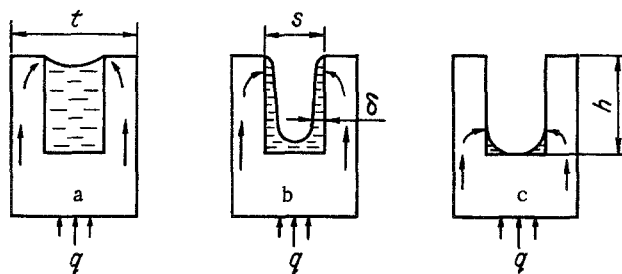


Fig. 3. Phases of the evaporative-pulsating regime: a) channel filled; b) deepening of the meniscus; c) partial dry-out of the channel.

wedge, the practical absence (sic) at the surfaces of the transport zone, and capillary feed of the working section (dimensions 30×30 mm) from an arterial grid. A specific pulsating regime was clearly observed in the experiments which was completely unlike the regime of which a description is given in [5, 13, 16]. The liquid from the arteries entered the channels in turn in portions with frequencies of the order of 0.2-0.5 Hz. It created the impression that jets of liquid were "launched" from the cells of the arterial grid in turn into the various channels. The general behavior of this regime of vaporization was retained up to a heat flux q_k , which was determined by the characteristic break-point on the boiling curve. The effective thermal conductivity of the channel in the evaporative-pulsating regime is practically independent of the value of the heat flux (Fig. 2). The value of q_k depends on the heat transfer medium, the saturation pressure, and the characteristics of the heating surface, and amounts to $(7.5-10) \cdot 10^4$ W/m² for water and $(2.5-3.5) \cdot 10^4$ W/m² for ethanol.

The observations provide a basis for assuming that similar regimes are possible for specific hydrodynamic interactions of the flows in the grooves and the arteries. Such interactions become more probable the smaller is the resistance of the grooves compared with the resistance on leaving the arteries. Similar regimes could exist in the well-known experiments of Morits [6]. At high heat-flux densities the periodic supply of liquid into the grooves cannot cause significant pulsations in the wall temperatures. This appears to be the most natural explanation of the experimental facts established in [6].

In order to develop a physical concept of the possible heat-transfer mechanism in the evaporation-pulsating regime considerable importance must first be placed on answering the question of what is the nature of the transfer of heat from the wall to the interface, and in particular whether its behavior can be regarded as a steady-state process either here or elsewhere in the unsteady-state process as a whole. For a preliminary analysis it is convenient to make use of the Fourier number Fo as an estimate of the time scale. As the characteristic dimension it is natural to select the thickness of the liquid layer whose thermal resistance governs the resistance to heat transfer under steady-state conditions.

Let us now consider the picture of the heat flow lines for wetted grooves (Fig. 3). It can be seen that the main transfer of heat occurs in narrow zones (in the corners), the scale of which is 10-100 times smaller than the width of the groove. Bearing in mind the specification that $Fo > 100$, i.e., that to a first approximation, even for unsteady-state processes such as occur in the evaporative-pulsating regime, the heat-transfer regime can be regarded as a quasi-steady-state process for each characteristic stage within which the shape and dimensions of the part of the groove wetted by the liquid are approximately retained (Fig. 3).

This concept, together with an analysis of the boiling curves and the models [17, 18], made it possible to carry out an evaluation of the experiments performed in the OTIPP for the evaporative-pulsating regime and the corresponding literature data (Table 2). All the points (Fig. 4) were correlated to an accuracy of $\pm 50\%$ by the equation

$$Z = q \sqrt[6]{\frac{v_L d^5}{r \sigma \lambda_m^2 \lambda_L^3 (1 - \epsilon)^5}} = 0.034 (\Delta T - \Delta T^*)^{5/6}, \quad (8)$$

where ΔT^* is the superheat caused by the curvature of the meniscus:

TABLE 2. Experimental Data on Heat Transfer During Vaporization in Capillary Channels

Working section	s	t	h	Heat-transfer medium	Heat flux, kW/m ²	Literature source	
Plates with rectangular channels							
A12	0,28	2,04	1,05	NH ₃	3,5	[11]	
A13	0,5	1	0,8	C ₂ H ₅ O	6—22,4	[9]	
A14	0,06	0,23	0,18	C ₆ H ₆	4,7—9,2	[12]	
A16	0,09	0,26	0,08	R12	1,77—3,8	[12]	
M4	0,05	0,55	0,4	R11	52—100	[19]	
M5	0,05	0,55	0,4	R11	1,4—190	[19]	
M6	0,25	1,35	1,25	R11	5—20	[19]	
M7	0,25	0,5	0,2	H ₂ O	2,2—4,45	[12]	
Working section	s ₀	s	t	h	Heat transfer medium	Heat flux, kW/m ²	Literature source
Plates with trapezoidal channels							
A10	0,9	0,66	1,2	1,02	NH ₃	2,6—2,9	[20]
A10	0,9	0,66	1,2	1,02	R21	0,56	[20]
A11	0,86	0,66	1,2	1,08	NH ₃	2,87	[20]
A15	0,12	0,2	0,35	0,46	R12	4—15	[12]
Working section	s	h	Heat transfer medium		Heat flux kW/m ²	Literature source	
Plates with triangular channels							
M8	0,5	0,1	R22		3,4—40,6	[21]	
M9	0,5	0,16	R22		3,4—46,4	[21]	

Note. On surfaces A12, M4, M5, M6, the complex channel profile was close to rectangular.

$$\Delta T^* = \frac{4\sigma T_s}{\mu \rho_V s}; \quad (9)$$

ϵ is the porosity, which is equal to 0.5 for the triangular channels and s/t for the rectangular channels; d is the characteristic dimension of the capillary channel, which is given for the triangular, rectangular, and trapezoidal channels respectively by:

$$d = \sqrt[5]{s \left(\frac{t}{4}\right)^4}; \quad d = \sqrt[5]{s \left(\frac{t-s}{2}\right)^4}; \quad d = \sqrt[5]{s \left[\frac{t-0,5(s+s_0)}{2}\right]^4}. \quad (10)$$

The use of relationship (8) for evaluating the experimental data of [22], which were obtained during the irrigation of vertical profiled surfaces, gave values of Z which were 1.5 times too large, which is probably explained by the absence of the drying phase in the grooves.

The boiling regime was observed when $q > q_k$. As the heat flux increased during the boiling of water there was immediately the appearance of individually acting centers of vaporization, the liquid became turbulent, and the wettability of the entire surface improved. The ejection of individual droplets began; after reaching a height of 0.2 m the droplets fell back onto the ribs and into the channels. The scale of the ejection depended on the width of the channel and on the thickness of the liquid layer on its surface. Thus, on the parts far from the arteries of the network the ejections were in the form of fine droplets. With ethanol at low pressure (0.025 MPa) on the plate Cl, the surface of which was well finished, no bubble boiling was observed. As the heat flux increased, centers of boiling appeared in individual grooves from which the liquid was ejected in the form of jets. At the same time, laminar flow of the liquid continued in the adjacent channels in which there were no centers of boiling. At a pressure of 0.1 MPa the ejection of the liquid from this same surface was observed in the form of individual droplets, and not in the form of jets.

When $q > q_k$ the effective thermal conductivity of the channel was larger than in the evaporative-pulsating regime and depended significantly on the value of the heat flux (see

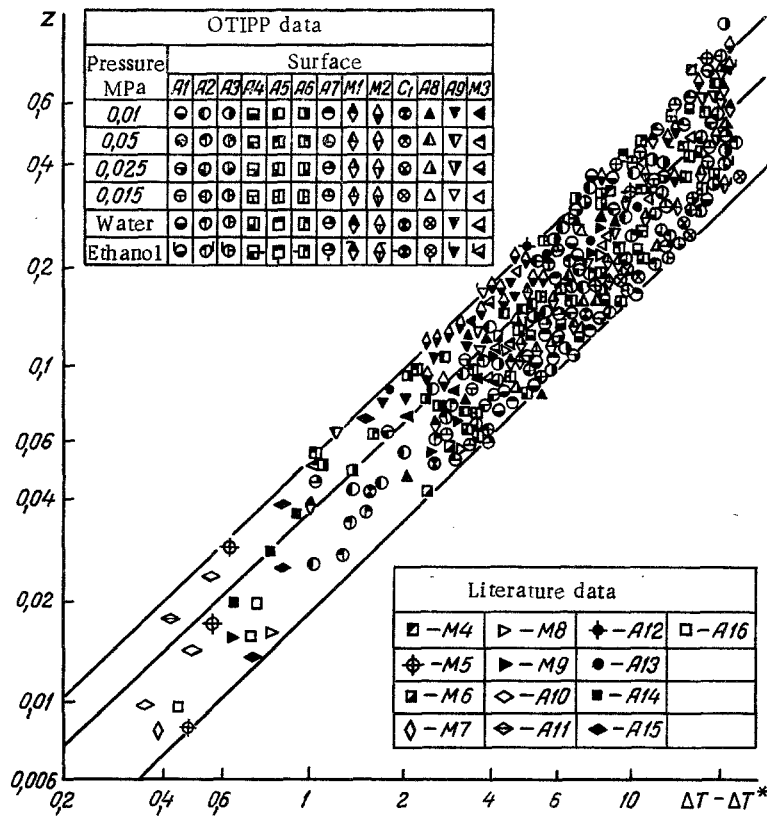


Fig. 4. Generalization of the experimental data. Evaporative-pulsating regime. $\Delta T - \Delta T^*$ in $^{\circ}\text{K}$.

Fig. 2). The type of heat transfer medium had a decisive effect on heat transfer, as well as the pressure, the thermophysical properties of the material of the surface, and the specific heat flux. The effects of the porosity and roughness of the surface were considerably smaller.

For evaluating the results the well-known model of microlayer evaporation of D. S. Labuntsov [23] was used as a starting point, on the basis of which a generalization of the experimental data was made (Fig. 5) for the surfaces being investigated (which were produced by mechanical means):

$$q = C_2 \left(\frac{\rho_v}{\rho_L - \rho_v} \right)^{0.3} \frac{\lambda_L \Delta T^2}{\sigma T_s} \left(\frac{\lambda_L \Delta T}{v_L} + 5r\epsilon_v \right).$$

The coefficient C_2 takes into account the properties of the material of the heating surface and of the heat-transfer medium. For the boiling of water on the copper, aluminum, and steel surfaces, C_2 was equal, respectively, to 4.42, 3.34, and 0.67, while for the boiling of ethanol, it was equal to 1.54, 2.42, and 0.7.

In the presence of a transport section whose length was comparable with that of the channel in the cooler, stabilization of the flow in the channels occurred. Under these conditions the specific features of heat transfer were determined by the interdependent nature of the heat-conduction processes in the film-wall system. The evaporators without feed arteries operated under these conditions (for example, grooved heat pipes without feed arteries); it is recommended that heat transfer in these be calculated according to Eqs. (1), (2).

In arterially grooved evaporators the pulsating nature of the irrigation of the channels does not lead to dry-out of the walls, and as a result, in these evaporators the intensity of heat transfer increases continuously with increase of the heat flux until the structures begin to steam (see Fig. 2). The main mechanism of heat transfer under these conditions is heat conduction from the wall to the interface, but the position of the interface is unstable, which makes it difficult to use equations (1) and (2) for calculations. The relationship (8)-(10) can be recommended for the thermal design of such evaporators, and particularly for the arterially grooved tubes.

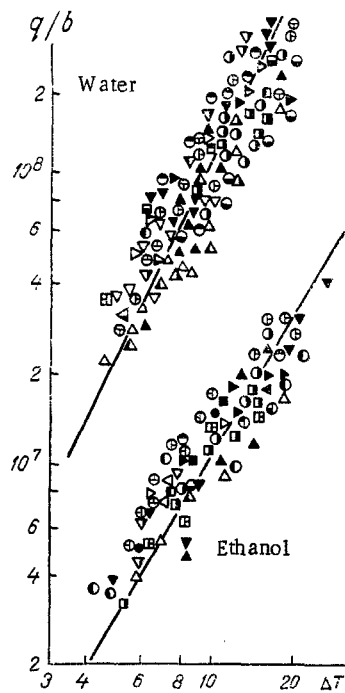


Fig. 5. Generalization of the experimental data. Boiling regime. (For explanation of the data points, see Fig. 4.) $B = [\rho_V / (\rho_L - \rho_V)]^{0.8}$. q/b is given in W/m^2 , and ΔT in $^{\circ}K$.

NOTATION

π , Perimeter of channel; Fo , Fourier number; P , pressure; ΔT , difference between wall and saturation temperatures; R , radius; Q , heat flux; q , heat flux density (q_{loss} = loss to surrounding medium); f , free cross-section of stream (f_0 = value in flooded channel); j , liquid flow rate; c , specific heat capacity; c_f , resistance coefficient due to friction; w , velocity; r , latent heat of vaporization; x , coordinate; s , h , l , width, depth, and length of channel; t , pitch between channels; n , number of channels; λ , thermal conductivity; α , angle of triangular channel; β , angle of inclination of the heating surface; ϵ , porosity; g , free-fall acceleration; μ , dynamic viscosity; ν , kinematic viscosity; σ , surface tension; ρ , density; d , characteristic dimension. Subscripts: L , liquid; M , metal; e , effective; s , saturation; v , vapor; k , boiling; o , basis.

LITERATURE CITED

1. K. T. Feldman and T. E. Berger, Technical Report ME-62(73) ONR-612-2, University of New Mexico (1973), pp. 13-18.
2. Y. Kamotani, AIAA Paper No. 147 (1976), pp. 1-9.
3. L. L. Vasiliev and A. N. Abramenko, in: Proc. Internat. Heat Pipe Conference, Bologna (1976), pp. 463-472.
4. L. L. Vasiliev, A. N. Abramenko, and S. V. Konev, in: Proc. Internat. Heat Transfer Conf., Toronto, Vol. 1 (1978), pp. 299-304.
5. K. S. Frank, Intersociety Energy Conversion Conference, ASME (1967), pp. 833-846.
6. K. Moritz, Heat Pipes [in Russian], Moscow (1972), pp. 33-117.
7. V. Ya. Sasin, B. R. Temkin, and A. I. Arkhipov, Tr. MĖI, No. 12, 159-164 (1976).
8. L. L. Vasiliev, A. N. Abramenko, and L. E. Kanonchik, Inzh.-Fiz. Zh., 39, No. 3, 449-457 (1980).
9. V. L. Barantsevich, S. I. Opryshko, and V. Ya. Sasin, Tr. MĖI, No. 560, 40-46 (1982).
10. V. A. Babenko, L. P. Grakovich, M. M. Levitan, et al., Heat Transfer in Cryogenic Devices [in Russian], Minsk (1979), pp. 3-13.
11. W. Harwell, W. B. Kaufman, and L. K. Tower, AIAA Paper No. 773, 1-8 (1977).
12. C. C. Roberts, AIAA Paper No. 75-724, 1-11 (1975).
13. V. Chaikovskiy, Z. Smirnov, and O. Burdo, in: Proc. Internat. Heat Pipe Conference, Palo Alto, No. 78-460, 426-433 (1978).
14. O. G. Burdo and Zh. B. Smirnova, Inzh.-Fiz. Zh., 40, No. 3, 535-536 (1981).
15. O. G. Burdo, Zh. B. Smirnova, O. B. Bin'kovskii, and Van Chang Le, Kholodil'naya Tekh. Tekhnol., No. 38, 30-34 (1984).
16. V. G. Voronin, A. V. Revyakin, and V. S. Tarasov, Voprosy Radioĕlektron., Ser. TRTO, No. 2, 21-27 (1974).

17. G. F. Smirnov, *Teploenergetika*, No. 9, 77-80 (1977).
18. O. N. Man'kovskii, O. B. Ioffe, and L. G. Fridgant, *Inzh.-Fiz. Zh.*, 30, No. 2, 310-316 (1976).
19. W. Nakayama, Proceedings of the 7th International Heat Transfer Conference, Munich, Vol. 1 (Sept. 6-10, 1982), pp. 223-240.
20. P. I. Brennan, E. I. Kroliczek, H. Ien, and R. McIntosh, AIAA Paper No. 77-747, 1-9 (1977).
21. I. Masaaki, *Bull. JSME*, 22, No. 171, 1251-1257 (1979).
22. D. K. Khrustalev, "Procedures for calculating the heat transfer characteristics of low-temperature heat pipes with open longitudinal capillary channels (channel type)," Author's Abstract of Candidate's Dissertation, Technical Sciences, Minsk (1984).
23. V. A. Girgor'ev, Yu. M. Pavlov, and E. M. Ametistov, *The Boiling of Cryogenic Liquids* [in Russian], Moscow (1977).

HEAT TRANSFER IN THE LAMINAR-WAVE SECTION OF CONDENSATION OF A
STATIONARY VAPOR

V. M. Budov, V. A. Kir'yanov,
and I. A. Shemagin

UDC 536.423.4

A method is proposed that specifies and refines the relation for the average coefficient of heat transfer at $Re \leq 250$.

The oscillatory motions of a phase interface resulting from the development of wave flow of a condensate film determine the intensification of heat exchange during condensation on a vertical surface [1-3].

In the existing methods of calculating the average coefficient of heat transfer in the laminar-wave section, wave formation is taken into account by the introduction of a correction factor to the Nusselt equation in the form of a constant [2] ($\overline{Nu}/\overline{Nu}_N = 1.21$) or a certain function of the Reynolds number [3]:

$$\overline{Nu} = 0.95 Re^{0.04} \overline{Nu}_N \quad (1)$$

The relation (1) has found wide popularity, despite the fact that it was confirmed experimentally only for low Reynolds numbers $Re \leq 40$ [4]. The cycle of experimental research presented in [5] revealed an excess of the experimental data at $Re > 40$ over the values found from (1), increasing with an increase in the Reynolds number. This disagreement is connected with the fact that in (1) the correction to the Nusselt equation for wave formation refers to the entire heat-exchange surface, containing both the wave section of condensate flow and the purely laminar section, in which intensification of heat exchange does not occur.

The authors propose to refine the above method of calculating the average coefficient of heat transfer (1) by the introduction of a correction factor allowing for the intensification of heat exchange only in the wave section.

Thus specifying the expression for \overline{Nu} , we obtain

$$\overline{Nu} = L^{-1} \left[\int_0^l Nu_N(x) dx + \varepsilon_w \int_l^L Nu_N(x) dx \right] = \overline{Nu}_N \left[\left(\frac{l}{L} \right)^{3/4} + \varepsilon_w \left(1 - \left(\frac{l}{L} \right)^{3/4} \right) \right], \quad (2)$$

where ε_w is the correction for wave formation, the value of which is determined by the Reynolds number, as was shown in [3].

The dependence of the coordinate of the start of development of the wave regime (l) on the parameters of the condensation process is determined from an analysis of the stability of laminar flow of the condensate film. From the results of such an investigation [6-8] for the

A. A. Zhdanov Polytechnic Institute, Gor'kii. Translated from *Inzhenerno-Fizicheskii Zhurnal*, Vol. 52, No. 6, pp. 907-909, June, 1987. Original article submitted February 25, 1986.